Deposits of Sand: Ripples Versus Dunes

5

We have seen that sediment can form mounds on the surface and that these mounds can grow through the instability associated with the saturation length. However, several effects lead to more complex structures—the recirculation bubble of airflow, the avalanching slip face of the dune, and the possibility that multiple particle sizes or densities may be present. These lead to some distinct types of structures—ripples rather than dunes. The way sediment is deposited can also leave traces in the dune (or in a sandstone if the dune becomes lithified), or on the surface on which the dune sits.

5.1 Flow Separation and Recirculation

First, airflow going around a surface will try to follow it. However, like tea poured from the spout of a well-designed teapot, if the surface peels away too sharply, the airflow cannot follow it and detaches from it. This flow separation means the lee side of the dune can be rather sheltered, experiencing much less wind stress. Often there is a recirculating flow behind the dune, in the so-called separation bubble, before the airflow re-attaches downwind. This recirculating vortex leads to a reverse flow on the lee side, which can sweep sand back towards the dune. This recirculating vortex and its role in dune dynamics was recognized over a century ago (Cornish 1897).

This recirculation can be studied with field instruments, or visualized with smoke or streamers (e.g., Fig. 5.1), or sometimes shown by the sand itself. It has also been studied in wind tunnels and with computer simulations (Fig. 5.2; Schatz and Hermann 2005; Hermann et al. 2005; see also Chap. 19). Occasionally, the sand itself acts (imperfectly) to visualize the flow, as saltating sand flies off the crest of a saltating dune (Fig. 5.3). Typically, the reattachment point is downwind of the dune toe by 4–6 times the dune height, although a wider range may be encountered depending on the surface roughness upwind, and the sharpness of the separation point.

The recirculating flow can sweep sediment back towards the slip face of the dune if the floor is smooth. The separation bubble can strongly influence how dunes mutually interact, notably in the case of barchans—once the downwind barchan enters the lee of the upwind one, the airflow on it will be considerably disturbed.

5.2 Angle of Repose: The slip face

The second effect involves the sand, whether or not an atmosphere is present. Sand generally has small cohesion, and the sideways forces at sand–sand contact surfaces is due to friction alone. This means that a pile of sand will tend to have slopes that do not exceed the angle of repose—in fact, when granular materials, whether sand, gravel, cobbles, or boulders, come to rest on or adjacent to comparable particles, they tend to form piles with uniform slopes. If sand is added to the top of a pile or slope, it may steepen initially, but soon an avalanche will occur, where the weight of sand has overcome friction and allows the sand to move until the slope has shallowed to the angle of repose once more. The progressive deposition of sand on the lee side of a dune means that the lee side sees continual avalanching and is generally at the angle of repose.

For well-rounded, dry sand grains, the angle of repose is around 33°. Accumulations of irregular coarse particles (pebbles or cobbles) can attain an angle of repose of 41°, but such a slope is not typical for sand accumulations that do not also include a considerable quantity of silt or clay. The strength of the acceleration of gravity is not a prominent factor in determining the angle of repose, which is more dependent upon systematic trends in particle shape or particle surface roughness. Since the angle of repose is weakly diagnostic of grain shape, constraints on the latter

R. D. Lorenz and J. R. Zimbelman, *Dune Worlds*, Springer Praxis Books,
DOI: 10.1007/978-3-540-89725-5_5, © Springer-Verlag Berlin Heidelberg 2014

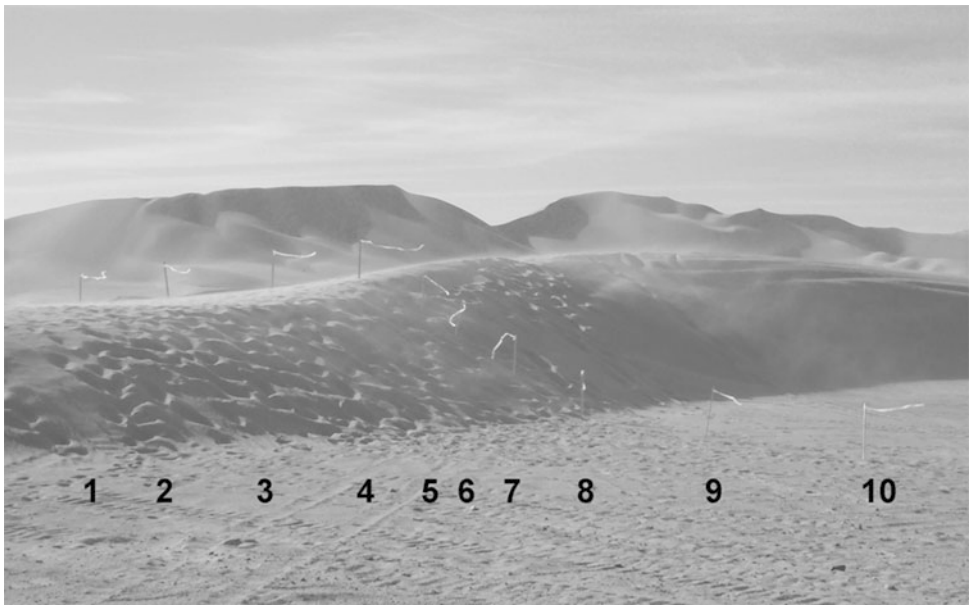

Fig. 5.1 Streamers on a linear dune (no slip face) at the Dumont dunes, California. Wind is blowing from *left* to *right*, as shown by streamers on sticks at stations 1–4 (stakes are about 70 cm high). The strong *left–right* wind resumes at stations 9 and 10 where the flow has re-attached. At stations 5–8, the streamers droop, indicating low wind, and at stations 6 and 7 indicate an uphill flow due to the recirculating vortex in the lee of the dune. *Photo* R Lorenz

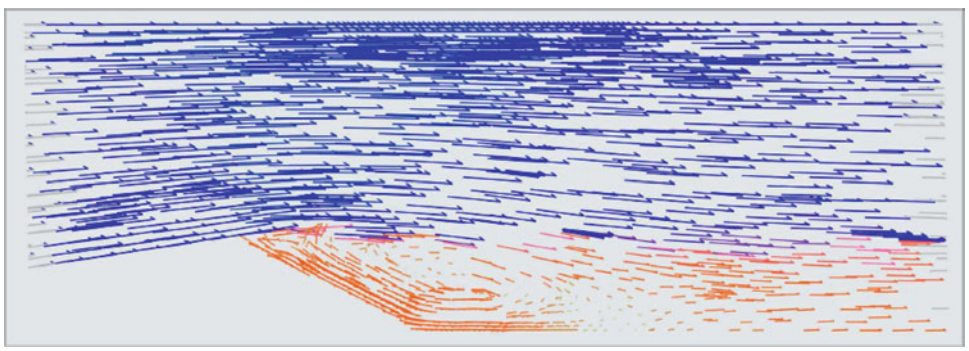

Fig. 5.2 Airflow vectors over a transverse dune, simulated using computational fluid dynamics (CFD—see Chap. 19) showing the flow separation at the crest and the recirculating vortex in the lee. (From Schatz and Hermann 2004, image courtesy of Hans Jurgen Herrmann.)

can be derived by measuring the angle, which is readily done by drizzling sand to form a conical pile. This experiment was performed (e.g., Moore 1987) by the sampling arm of the Viking lander on Mars in 1976 (see Fig. 5.4). Experimental studies have demonstrated that changing the strength of the acceleration of gravity has a minimal to non-detectable effect upon a dynamic angle of repose, as is the case within a rotating drum.

The grains on the slip face are usually loosely packed and thus have little cohesive strength. The combination of this weak packing and the steep slopes makes it difficult to climb the slip face on foot or in vehicles (see Sect. 1.4). On the other hand, it is easy to slide down—dune skiing and surfing is possible (Fig. 5.5).

Because the entire slip face is essentially at the avalanching threshold, it is a 'critical' system wherein avalanches can take place over the whole size range from a single grain

Fig. 5.3 'Smoking dune': wind from *left* to *right* is launching sand which initially follows the separating streamline at the crest, but drizzles down in clouds onto the lee side. Lee deposits are thus often a layered combination of these airfall deposits and avalanche flows. See also Fig. 12.13. Dune near Palen: *Photo* J. Zimbelman

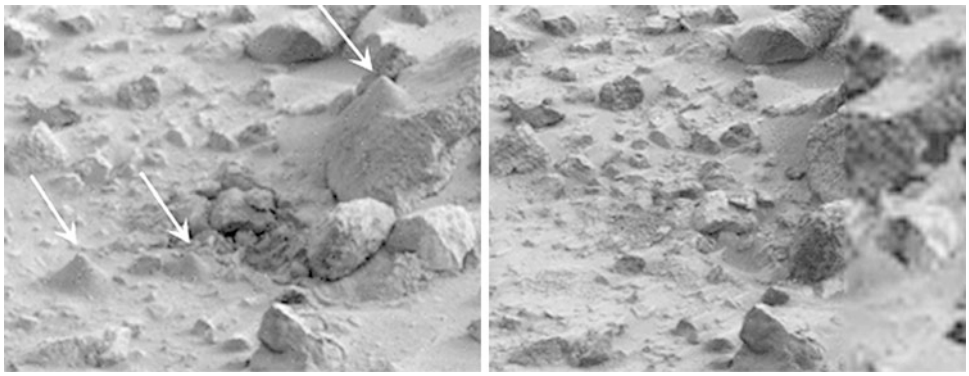

Fig. 5.4 Small conical piles of dirt (*arrowed*) created by the Viking Lander 1 sampling arm. The pile was made to estimate the angle of repose of the sediment, and to observe any changes. The image on the *left* was taken on Sol 921; the composite image on the *right* (where the sandpiles have been blown away) was assembled from images taken on Sols 2068 and 2209. This excellent comparison was assembled by Phil Stooke

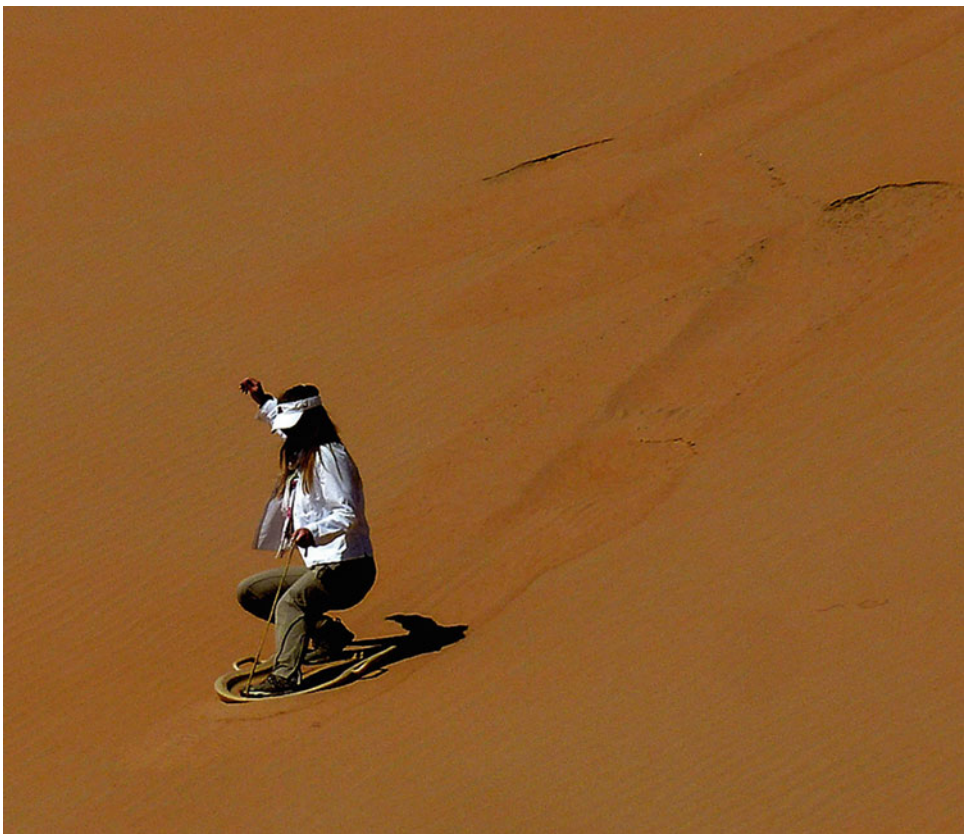

Fig. 5.5 The slip face of a dune can be steep and loose enough to permit rapid descent, as in this case (Jani Radebaugh dune-surfing on a megabarchan near Liwa in the United Arab Emirates). However, the friction is still rather higher than for snow, and the experience is not always totally exhilarating. *Photo* R. Lorenz

dropping one grain width, to the entire slip face sliding. It is found, both in reality and with computer simulations (see Chap. 19) that the relative frequency of avalanches varies as an inverse power law, with avalanches that are 10 times bigger occurring 10 times less often. The same sort of power law statistics are seen with earthquakes, forest fires, mountain avalanches and so on, and are studied under the physics umbrella of 'Self-Organized Criticality', e.g., Bak (1999).

Fig. 5.6 Lobe-shaped avalanches on the slipface of a barchan dune in the United Arab Emirates. The slip face is about 2 m high. The alcoves, with vertical gouges, from which the avalanching sand started are clearly visible—evidently some sorting results in the surface sand having a slightly different color. *Photo* Jani Radebaugh

Individual avalanches typically occur over fairly narrow spans of a dune, forming a narrow lobe (see Fig. 5.6). Avalanching is sometimes accompanied by a hissing sound, or sometimes much louder sounds and seismic vibrations (see Chap. 10: Booming dunes). Such avalanche lobes have been observed on Mars (e.g., Horgan et al. 2012; see Fig. 5.7).

5.3 Grain Sorting

A final issue is that sand can often be a mixture of materials or particle sizes. Since these are transported with different effectiveness by the processes of saltation and reputation for any given windspeed, they can be segregated, leading to different concentrations of them on different parts of an aeolian bedform. It is, for example, easy to observe that the crests of dunes often have coarser sand. The sorting is most evident on ripples, which often form (see Sect. 5.4) when fine sediment can be armoured by coarser grains. The coarse grains tend to accumulate on the upwind face, and especially the crest, of the ripples (e.g., Fig. 5.8). Exactly the same phenomenon is observed on Mars (e.g., Figs. 5.9 and 5.10)—see also Jerolmack et al. (2006).

The preferential accumulation is due to the reduced mobility of the larger particles. Similar differential mobility can result from grain size or the density of material from which the grain is made. This is often noticeable in terrestrial dunes, where the iron mineral magnetite is both appreciably denser than the quartz that makes up the bulk of the dune, but is also much darker and so accumulations are readily visible (Fig. 5.11). In the Namib sand sea, dark patches seen on dunes are concentrations of not only magnetite, but also ilmenite and garnet (e.g., Schneider 2008).

5.4 Dunes Versus Ripples

What is the difference between a ripple and a dune? Typically, but not always, there is a scale difference—ripples are small (e.g., Fig. 5.12). But the largest ripples on Earth can be as large as small dunes, and the distinction may blur even further on other worlds. Ripples do not have slip faces (and although no bigger than terrestrial ripples, it was the presence of slip faces on dunes formed under Venus-like conditions in a wind tunnel that led to the bedforms being called 'microdunes'—see Chap 14). However, since many dunes also lack slip faces, this is not a discriminator either. The challenge here is that the different terms are really genetic rather than purely morphologically descriptive. Both features are the result of sand grains being transported by the wind, but the processes involved in the formation of these two features are quite different. To avoid falling into the trap of misidentifying features on Mars without knowing

Fig. 5.7 Mars dune avalanching. Three images of the same location (taken by the High Resolution Imaging Science Experiment (HiRISE) camera on NASA's Mars Reconnaissance Orbiter) taken at different times on Mars show seasonal activity causing sand avalanches and ripple changes on a Martian dune. Time sequence of the images progresses from *top* to *bottom*. Each image covers an area 285 × 140 m. The crest of a dune curves across the *upper* and *left* portions of the image. The site is at 84° north latitude, 233° east longitude, in a vast region of dunes at the edge of Mars' north polar ice cap. The area is covered by carbon-dioxide ice in winter but is ice-free in summer. The *top* and *bottom* images show part of one dune about one Mars year apart, at a time of year when all the seasonal ice has disappeared: in late spring of one year (*top*) and early summer of the following year (*bottom*). The middle image is from the second year's mid-spring, when the region was still covered by seasonal carbon-dioxide ice

for sure how they formed, a new (if ungainly) morphological term was introduced: Transverse Aeolian Ridges (TARs—Fig. 5.13). To help better understand why a ripple is not just a very small dune, we must go back to what several researchers had to say about both ripples and dunes.

Bagnold (1941, p. 62) described a 'characteristic path' for well-sorted, wind-blown sand grains, which he argued was the result of momentum removed from the wind at the height reached by most of the saltating grains (see discussion above regarding wind profiles during saltation). He further argued that the wavelength of wind ripples (typically ~15 cm for simple ripples in fine sand, Fig. 5.12) is therefore the physical manifestation of the characteristic path of the wind-driven sand.

Sharp (1963) inferred that because aerodynamic (formed by the wind, as opposed to ripples formed by flowing water) ripples are observed to start off as small-amplitude, short-wavelength irregularities in a sand surface, which subsequently increase in wavelength as they evolve toward a steady state, Bagnold's 'characteristic path' concept for a wind ripple wavelength was suspect. Through geometric arguments, Sharp (1963) proposed the alternative concept that ripple wavelength depends on ripple amplitude and the angle at which the saltating grains approach the sand bed, so that ripple wavelength is controlled by the length of the zone shadowed (Fig. 5.14) downwind of the ripple from significant sand grain impacts, and also by the wind velocity that is the cause of the saltation action.

Anderson (1987) developed an analytical model for the initiation of sand ripples that result from the growth of perturbations on an initially flat sand surface. Using the 'splash function' concept derived from wind tunnel experiments by Unger and Haff (1987), Anderson (1987) modeled the wind tunnel measurements of relatively low-velocity ejection of grains caused by the impact of faster-moving saltating grains; he termed this splash process as 'reptation', from Latin for 'to crawl', to distinguish this mode of sand transport from saltation, suspension, and impact creep. Subsequent numerical modeling including both saltation and reptation (Anderson and Haff 1988) showed that small, fast-moving ripples overtake and merge with larger, slower ripples, resulting in the growth of the mean wavelength for the entire ripple field, along with a decline in the dispersion of wavelengths (that is, the observed range of wavelengths decreases as the ripple field evolves toward a steady state). Both reptation and saltation have been incorporated into subsequent continuum analytical models developed for the study of aeolian features on Earth and Mars (e.g., Momiji et al. 2000; Yizhaq et al. 2004; Yizhaq 2005), and numerical models (e.g., Landry and Werner 1994).

Bagnold (1941) described some important distinctions between ripple and dune formation processes: dunes usually display a slip face dominated by avalanche processes; ripples have the coarsest material collected at the crests with the finest material in the troughs, whereas the opposite is true for dunes. When aeolian sand is poorly sorted (that is, a wide range of particle sizes is present), the coarse grains become concentrated at the crests of large features that Bagnold (1941, pp. 153–156) termed 'ridges' rather than ripples, arguing that the coarse grains are moved by the impact of saltating sand. Other terms have been used to

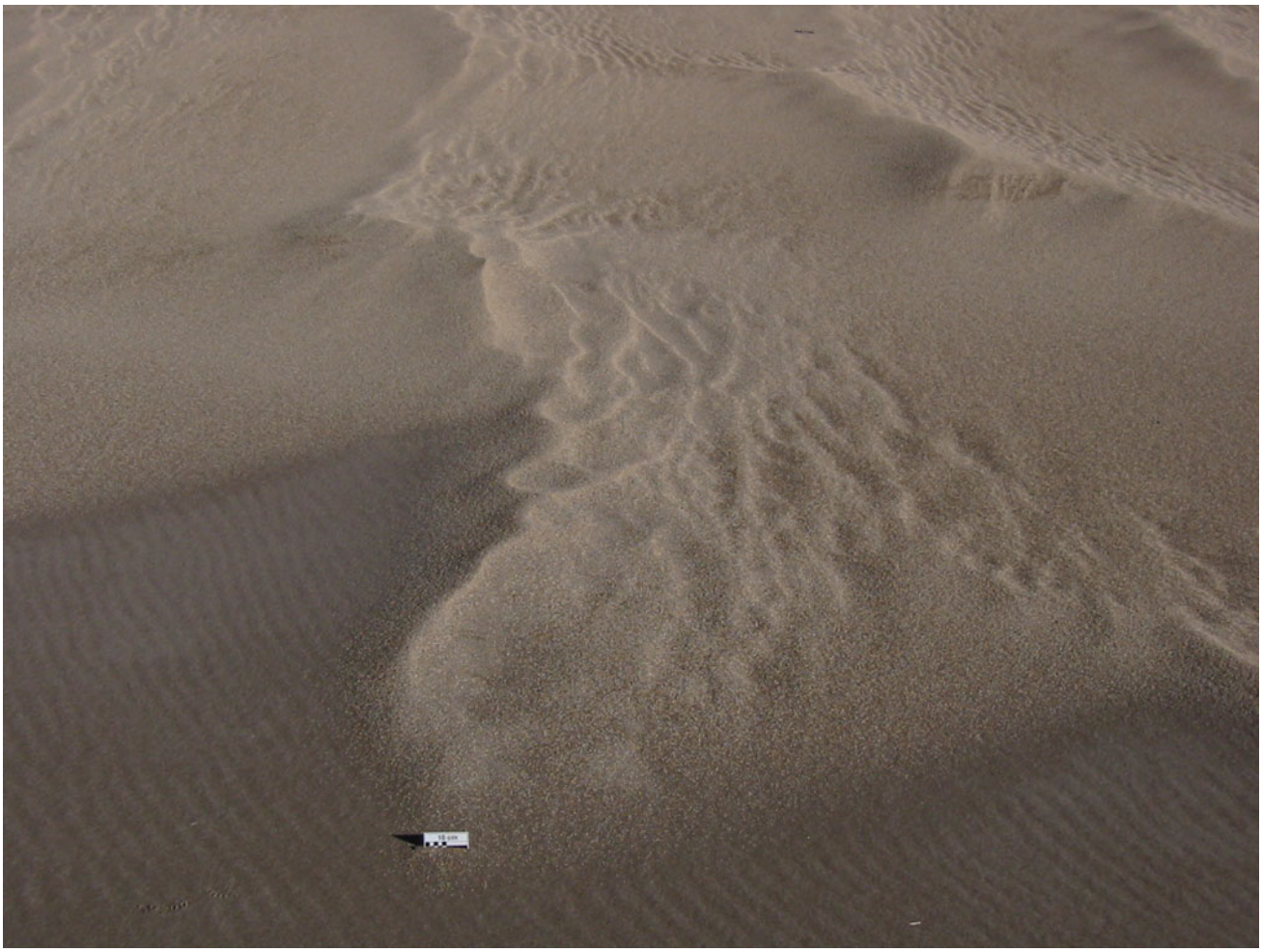

Fig. 5.8 Granule megaripples, with smaller accumulations of coarse granules on lee of each megaripple, Great Sand Dunes National Park and Preserve. Megaripples are coated by mm-sized granule particles. Normal aerodynamic sand ripples are encroaching onto the megaripples, from *lower left* in this view. Scale is 10 cm long. *Photo* J. Zimbelman

describe large wind ripples coated by coarse particles, but the term 'megaripple' is perhaps the one carrying the least interpretive 'baggage' with its use.

Sharp (1963) described 'granule ripples' as consisting of a surface concentration of grains >1 mm (Fig. 5.7), roughly equivalent to Bagnold's 'ridges'. Sharp concurred with Bagnold that impact creep, accompanied by significant deflation of the sand surface, was the dominant process involved in the formation of granule ripples. Ripples coated by coarse-grained particles can grow to great size; wavelengths of 20 m and heights of 60 cm are reported by Bagnold (1941, p. 155), and recently wavelengths of 43 m and heights of >2 m are reported for gravel-covered ripples in Argentina (Milana 2009; de Silva et al. 2011; see Fig. 5.15). More typically, granule ripples have wavelengths in the range of ~3 to 10 m and heights of ~25 to 40 cm (Sharp 1963; Zimbelman and Williams 2006; Zimbelman et al. 2012; see Fig. 5.7).

The coating of coarse particles, whether granules or gravel, tends to be concentrated at the surface of the bedform, usually as a monolayer of the larger particles, with the interior of the bedform comprised primarily of sand and only occasional coarse particles (Fig. 5.16). For granule ripples, the granules are most thickly accumulated at the crest of the ripple (Sharp 1963).

Profiles measured perpendicular to the crest of the features turn out to be valuable for distinguishing between aerodynamic sand ripples, megaripples, and sand dunes. Ripple profiles can be measured in the field from photographs (see Chap. 16)—a neat field trick is to use a straight edge to cast a shadow on the ripple surface. The profile shapes are distinct for each of the three classes of

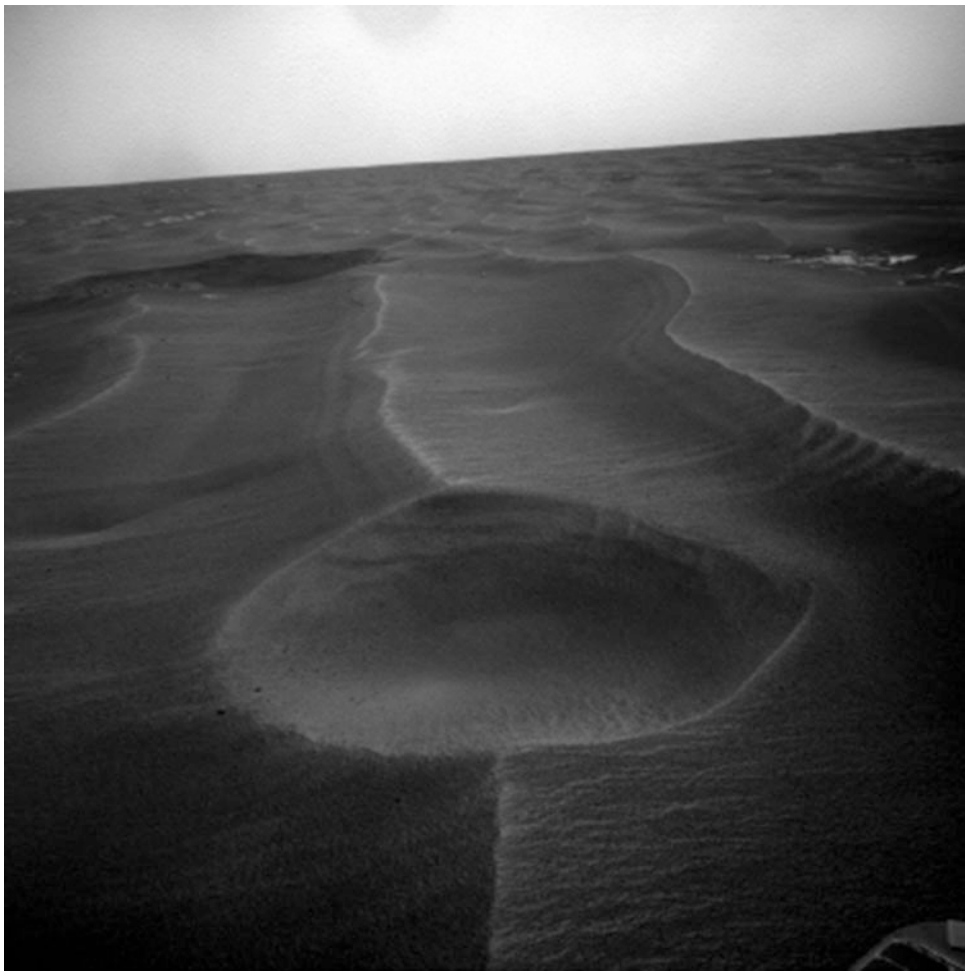

Fig. 5.9 Navcam image from the Opportunity rover of a small impact crater ('Rayleigh') which cuts into a ripple, neatly showing the cross-section of the ripple and exposing the angle of the layers in it. The intersection of the layers with the ripple surface can be seen behind the crater, and on the ripple to the *right*. *Image* NASA

features; when both the horizontal and vertical dimension are scaled by the width of the feature, profile shapes can be compared directly even for features that differ in scale by more than three orders of magnitude (Zimbelman et al. 2012; see Fig. 5.17). Profile shape can be assessed from remote sensing imaging data (see Chap. 18), and if combined with an assessment of the dominant particle size associated with a particular aeolian bedform, the probable formational mechanism involved in the development of both large ripples and small dunes should be identifiable even when detailed field examination may not be possible. Balme et al. (2008) show that at least some TARs observed on Mars have identical shapes to some wind ripples on Earth.

5.5 Controls on Feature Scale

We have discussed various factors controlling the scale of aeolian features: it is worth a brief recapitulation at this point. Ripples are defined by the shadow zone of saltating particles—it is somewhat similar to but not quite the same as the saltation path length. The ripple wavelength therefore relates to the windspeed (as demonstrated in wind tunnel experiments, e.g., Seppala and Linde 1978) as well as the particle size and other factors. The largest ripples form when the grains are coarse and thus can only be moved by the fastest winds, giving the longest saltation path length. Similarly, the long, shallow trajectories of grains on Mars yield large ripples or TARs. On the other hand, the saltation paths are short enough on Venus and Titan (Kok et al. 2012) that ripples may be insignificantly small.

The smallest ('elemental') dunes, on the other hand, are defined by the saturation length, which scales with the drag length. This in turn depends on the particle size, and the particle and atmospheric density, but does not depend on the windspeed. Dunes can grow in size, both by direct grain accumulation, and by coalescence with other dunes. However, dune growth ceases when the dune is large enough to 'feel' the top of the planetary boundary layer, which happens roughly when the dune spacing (typically six times the dune height) approaches the boundary layer thickness. Again, there is a consistent progression in size from Venus, through Titan then Earth, to Mars with the largest elemental

Fig. 5.10 Portion of a Curiosity MastCam image of a ripple surface, after a sample was scooped out. Note abundant fine brown sand exposed beneath mm-sized granule coating. Scoop is 4.5 cm wide. *Image* NASA/JPL

dunes. The same progression, more or less, arises for the largest dunes. The root cause is the same (atmospheric density), although the pathway is a little different: denser atmospheres take more heat to warm up by sunlight, so the thinnest atmosphere (Mars) has the thickest boundary layer and thus the largest dunes. The boundary layer depends on the thermal inertia of the surface, and on the length of the day, etc., so one could imagine a selection of exoplanets where the order of elemental dune size actually differs from the largest dune size.

Normal aerodynamic sand ripples are the smallest members in a hierarchy of aeolian landforms. Wilson (1972a, b) documented three distinct scales for aeolian landforms: ripples (wavelength 0.01–10 m), dunes (wavelength ~10–500 m), and draas (wavelength ~0.7–5.5 km) (Fig. 5.18). Note that Wilson's work includes both (small) sand ripples and (large) granule-coated ripples within the features he called 'ripples'; we will further explore this distinction shortly. A region of overlap exists between the measured dimensions of small sand dunes and large ripples, but the average sediment size of a 10 m dune is typically <0.2 mm while surface sediments on a ripple of 10 m wavelength are >1 mm, and importantly there are no observed transitional features between these two groups (Wilson 1972a). Therefore, particle size is an important characteristic of which class a 10 m-scale aeolian landform belongs to. Interestingly, the 10 m size of both large ripples and small dunes is comparable to the smallest aeolian features originally identified as TARs on Mars (Wilson and Zimbelman 2004). Features at all three length scales can be present at one location at the same time, but they are the result of differing wind intensities and durations (Wilson 1972b); this interpretation is consistent with the concepts presented by Sharp (1963), who stated that each aeolian bedform reaches its own quasi-equilibrium state; i.e., ripples do not grow to become dunes, nor do dunes grow to become draas (The Arabic word 'draa' means 'arm' and is often used to refer to megadunes, particularly linear ones, but also to compound dunes. Because a widely-accepted formal definition is lacking, we have tended not to use it).

5.6 Sedimentation and Dune Structure

The different modes of particle motion (suspension, saltation, reptation, creep) all deposit particles onto the surface in different ways. Suspended dust particles generally form a nearly uniform deposit without obvious layering. Large

Fig. 5.11 Compositional sorting. Eureka dunes, north of Death Valley National Park, showing concentrations of dense dark grains of magnetite. Thin lamellae of magnetite are exposed as rather pretty curves and loops in the slip face of the dune at *left*, with some patches of magnetite in the background. At *right*, differential concentration of magnetite grains on the sides of aeolian ripples on the dunes shows them much more starkly. *Upper right* inset: while jabbing eyeglasses into sand dunes is not generally a good idea, these ones have small magnets, which show clearly the magnetic nature of the dark grains. Photo by R. Lorenz

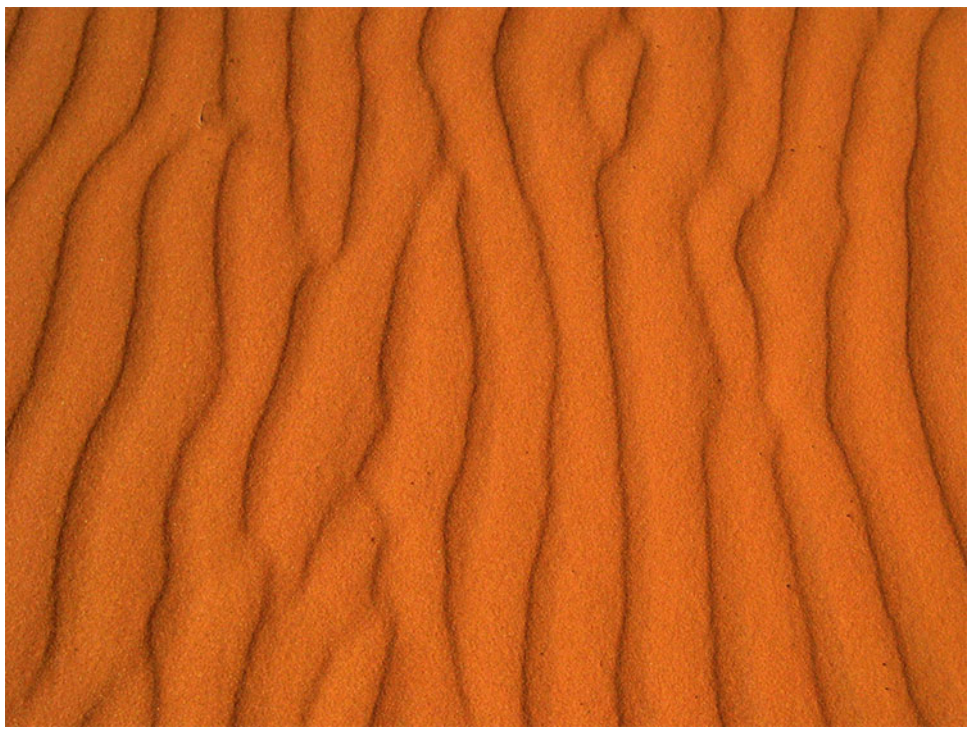

Fig. 5.12 Vertical view of typical aerodynamic ripples, coral pink sand dunes, State Park, Utah. Ripple wavelength is ~15 cm. Notice that while the pattern is quite regular, there are some defects forming Y-junctions (see Chap. 19). *Photo* J. Zimbelman

Fig. 5.13 Ubiquitous TARs seen on Mars. From the image alone, it is possible to infer that these are ridges and they are transverse (strictly the 'aeolian' in TAR is an assumption, though it seems safe to expect that this valley system has not seen water flowing for some considerable time). In all probability these are ripples in genetic terms, but TAR is a safer term. They are appreciably larger than typical ripples on Earth. MOC image (E02-02561) *Credit* NASA/JPL/MSSS

particles migrating via creep can accumulate within a sand deposit at locations that represent a former bedform, although stringers of coarse particles preserved within aeolian sandstone (in contrast to sandstone derived from sediment deposited by a river or other fluvial process) are surprisingly rare in the terrestrial geologic record (Sullivan et al. 2012). However, saltation and avalanching in dunes and ripples can lead to magnificent subsurface structures.

On the stoss side of a dune, grains are impacted onto the upward-sloping surface, and the grains tend to be packed (making it easier to walk on the stoss side). The wind on the sheltered lee side of the dune is weak, and the sand grains tend to be dropped by the airflow. The lee side of a dune under sand-driving winds experiences almost continuous slope failure in the form of numerous avalanches as discussed earlier.

Different episodes of deposition (e.g., seasonally-dependent winds) can result in distinct layers—usually distinct by means of different compaction and/or particle size (see pictures earlier in this section). Makse (2000) shows with a numerical model how cross-bedded layers can form due to the sorting by differential hop-length and rolling of different particle sizes or compositions. Dune slip faces can result in distinctively layered sand deposits (Fig. 5.19), some layering of which may represent the advancing slip face of an active dune. Traditionally, the layered structure of dunes was explored by sectioning or trenching the dune, sometimes with a bulldozer, although ground-penetrating radar can sometimes reveal such layering with less effort (see Chap. 18). In some circumstances the positions of former slip faces are exposed in the top surface of the dune, revealed either by cementation (Fig. 5.20) or by sorting (Fig. 5.21).

David Rubin of the U.S. Geological Survey has comprehensively mapped out via simulation how a growing layer of sand might record the style of deposition. In particular, when a repeating sequence of winds generates alternating episodes of slip face avalanching and ripple movement, a 3-dimensional record of layers is left in the resultant sandstone (Fig. 5.22). Usually only one, but sometimes more than one, section of this 3-dimensional pattern is exposed, in which case the interpretation can be non-unique. Rubin and Carter's (2006) animations of the growing pattern are a mesmerizing introduction to the richness of the patterns that can be found. The striking cross-bedded sandstones in Southern Utah (Fig. 5.23) are perhaps among the best-known examples of this aeolian deposition and lithification process. Some magnificent cross-bedding can also be seen in the sandstone into which the remarkable ancient city of Petra in modern Jordan was hewn: planetary geologists have been known to get more excited by its sedimentology than its archaeology!

The advent of very high resolution imaging from Mars rovers has now enabled similar cross-bedding textures to be found on that planet. The Opportunity rover studied Victoria Crater, a 750 m-diameter crater in Meridiani Planum, from 2004 to 2008 and observed stratified sedimentary rocks in the crater walls. As explored by Hayes et al. (2011) these layers chronicle the paleo-environments of Terra Meridiani and provide glimpses into the broader history of early Mars. The stratigraphy at Victoria Crater (Fig. 5.25) includes the best examples of meter-scale cross-bedding observed on Mars to date (Fig. 5.24). The Cape St. Mary promontory is characterized by meter-scale trough-style cross bedding, suggesting sinuous-crested dunes with scour pits migrating perpendicular to the outcrop face.

Finally, another deposit type can form in certain cases, where the sand is easily cemented. This is particularly the case for gypsum. Rain can cement gypsum sands to form a resistant layer: this will prevent movement for some time until the layer is broken up. However, where the layer intersects the substrate surface it may be preferentially preserved, leaving a surface scar that marks the perimeter of the dune. These can be seen in some instances at White

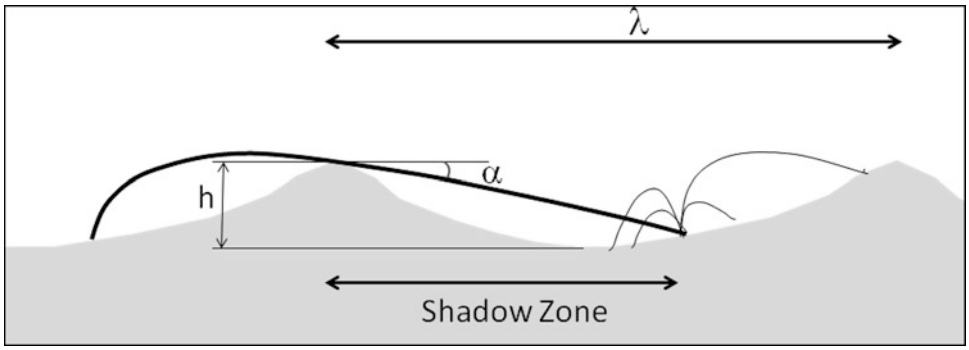

Fig. 5.14 Shadow definition of ripple wavelength λ. For a given windspeed, the impact angle α will be roughly constant, and so will the aspect ratio h/λ: over time, ripples may grow in both height and wavelength. In faster winds (e.g., on Mars), the angle α will be shallower, and longer wavelength bedforms result. The *solid line* shows a saltating particle (note that λ is defined in part by the length of the shadow zone and is related to, but not equal to, the saltation pathlength). The *thin curves* show typical 'splashed' particle trajectories

Fig. 5.15 Some of the largest ripples on Earth: the pumice gravel-coated megaripples, Perulla, Argentina. See Milana (2009) and de Silva et al. (2012) for further discussion of these megaripples. Shan da Silva for scale. *Photo* J. Zimbelman

Fig. 5.16 Concentration of cm-sized pumice clasts on the surface of a megaripple, Purulla, Argentina. The interior of the megaripple consists almost exclusively of medium sand derived from several ignimbrites exposed in the area; here particles from on the crest consistently fell onto the exposed trough dug across the ripple crest. Scale is in cm. *Photo* J. Zimbelman

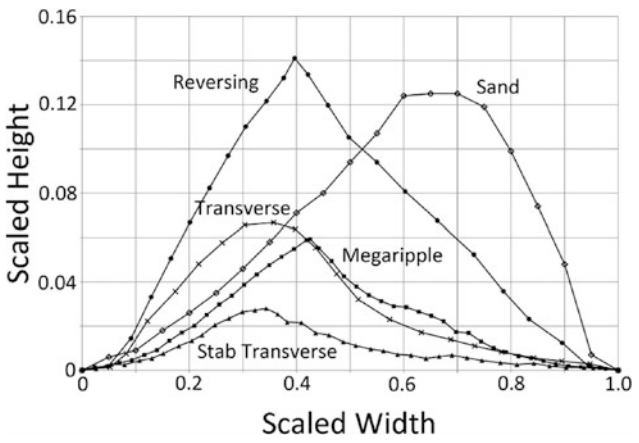

Fig. 5.17 Scaled profiles of different types of ripple (after Fig. 6 of Zimbelman et al. 2012)

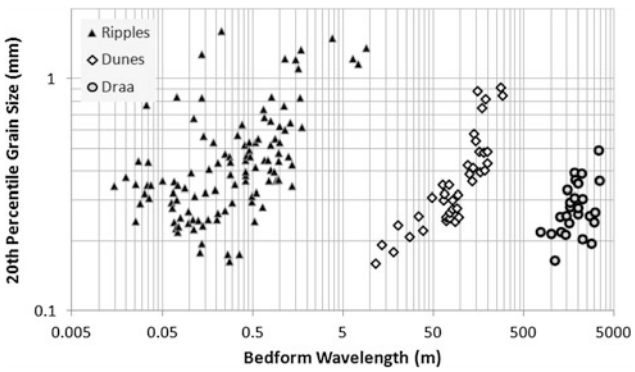

Fig. 5.18 Plot demonstrating three distinct scales of aeolian features showing data from Wilson (1972a). Points represent measurements of features from around the world—the three sets of points are quite distinct. *Vertical axis* is the grain size of the 20th percentile of particles from the feature

Fig. 5.19 Crossbedded layers in a dune exposed by digging: note the near-horizontal layers at *top*, and dipping slipface layers below. Ruler is 15 cm long (see also the boots at *upper right* for scale). *White* Sands National Monument, at the first Planetary Dunes workshop in 2008. Photo courtesy of Jani Radebaugh

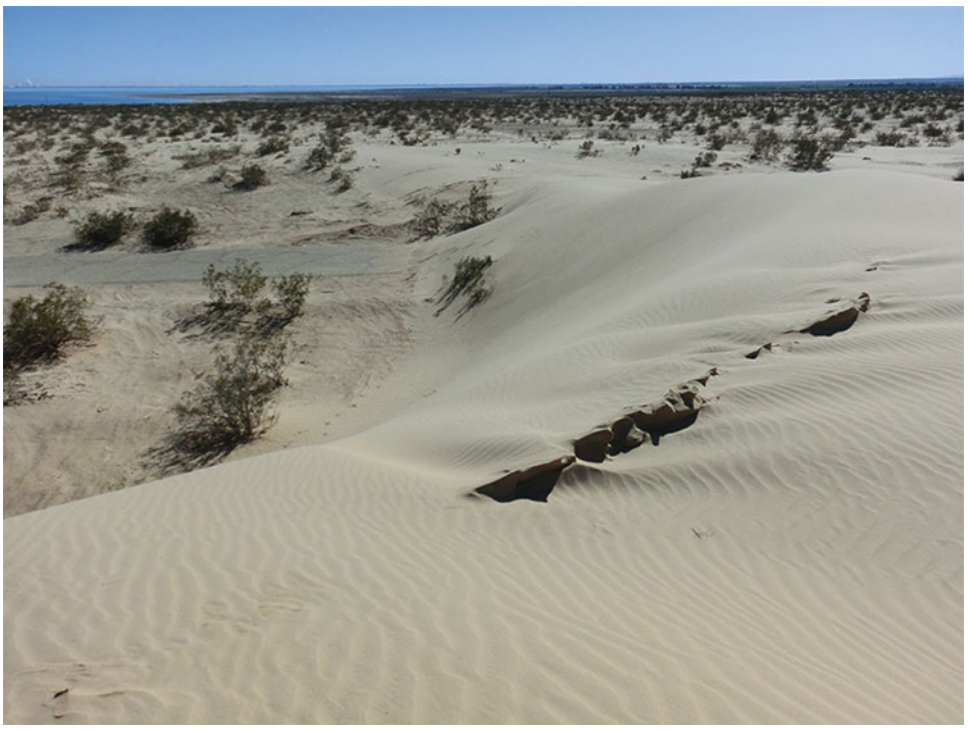

Fig. 5.20 Exposed cemented layers of a former slipface on a barchan near the Salton Sea (visible at *top left*) in Southern California. View is looking along one arm of the barchan, which has crossed and blocked a small road. *Photo* R. Lorenz

Fig. 5.21 Exposed layers in the damp sand of Lencois Maranhenses (a lagoon is just visible at *top left*) showing the arcuate former positions of the slipface of the barchanoid dunes. Jani Radebaugh for scale. Some wavy elemental dunes are forming in the background as the bright sand starts to dry and organize. *Photo* R. Lorenz

Fig. 5.22 Simulations of bed formation by Dave Rubin of the USGS show that the bedding pattern contains rich information that maps to the sequence of deposition styles. In this example, dunes form layers with additional complexity from along-crest migrating superimposed bedforms. The bedforms have a height ratio of 0.45 and a speed ratio of 0.3. The resulting ratio of along- to across-crest transport is 0.135; the transport direction is oriented 82° from the crestline of the main bedforms. *Image* USGS

Fig. 5.23 Cross-bedded Jurrasic sandstone in Zion National Park, Utah. Fine-scale layers represent sand deposited upon a sand dune, while the larger sets of layers, ranging from 2 to 12 m in height, record the passage of multiple sets of sand dunes. *Photo* J. Zimbelman

Sands National Monument (Fig. 5.26). Recently, high-albedo features (Fig. 5.27) seen at an equatorial dune field on Mars have been interpreted (Gardin et al. 2011) to be analogous to these White Sands 'barchan scars'. This is noteworthy since it would imply the existence of liquid water (perhaps from the subsurface) in amounts and for durations enough to cement the sand at the foot of the slipface.

5.7 Niveo-Aeolian Processes

An interesting complication can occur with sand dunes in cold regions on Earth in that both snow and sand can be present. Once snow falls under conditions that it is cold enough not to be sticky, it can be saltated, perhaps mixed with sand, forming intricate multiple layers (Fig. 5.28). Subsequently, further saltation may bury the snow under more sand.

The burial of snow by sand can both insulate the snow from heat, and retard the diffusion of moisture, allowing the snow to persist inside the dune. Depending on the temperature history, the snow may melt, moistening the sand and reducing its mobility (Fig. 5.29). This moisture may then refreeze, forming a very hard, cemented layer. On the other hand, if the dune accumulates rapidly, the snow may be preserved for long periods with no melting at all, and very slow sublimation if any. One example, in the Killpecker dune field in Wyoming, showed 25 cm-thick lenses of snow 1.5 m beneath the surface of a dune, some 4 months after

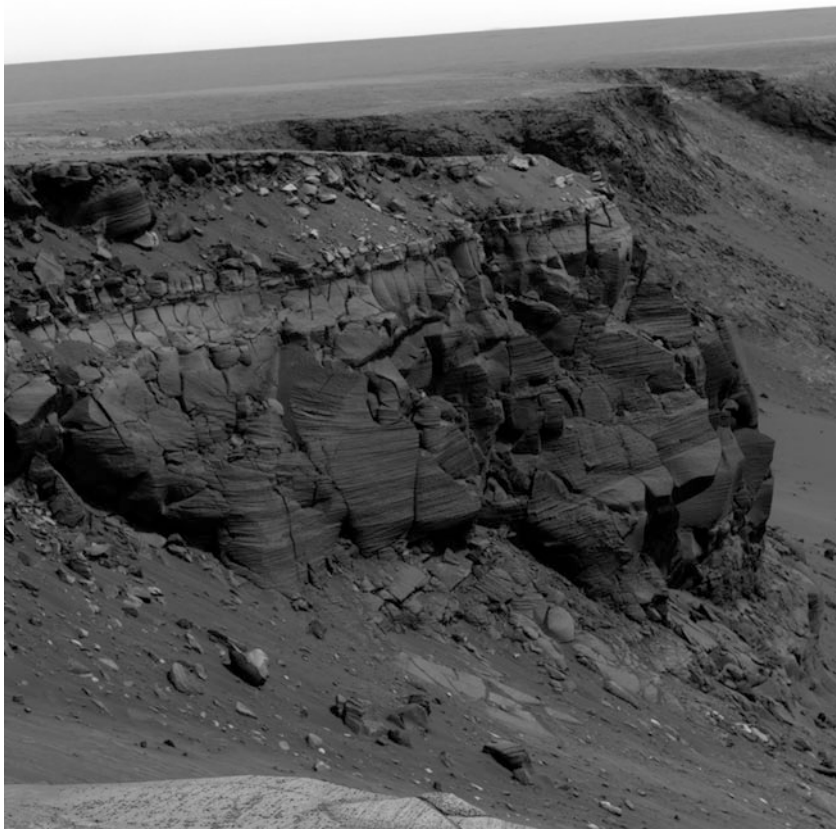

Fig. 5.24 Crossbedding on Mars. Opportunity mosaic of the Cape St. Vincent promontory on the edge of Victoria crater in Meridiani Planum, showing impressive layers in aeolian sands. Image courtesy of Alexander Hayes

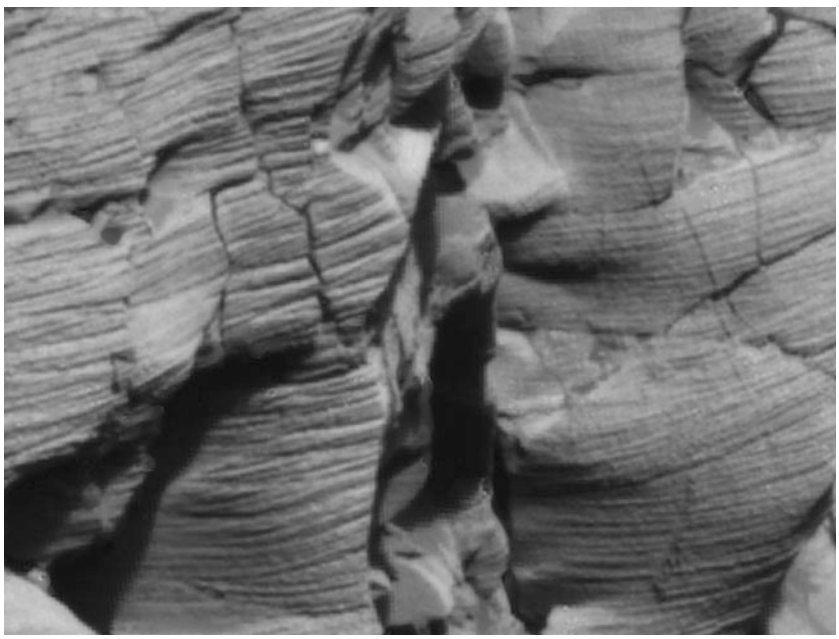

Fig. 5.25 A close-up of more layers in the walls of Victoria crater, this time at Cape St. Mary. Image courtesy of Alexander Hayes

Fig. 5.26 Arcs 0.5–1 m apart are fossil positions of barchanoid slip faces at White Sands National Monument, New Mexico, USA. The slip face position has been marked by cementation by moisture before the dune moved on. These scars are best seen with the sun low in the sky. *Photograph* R. Lorenz

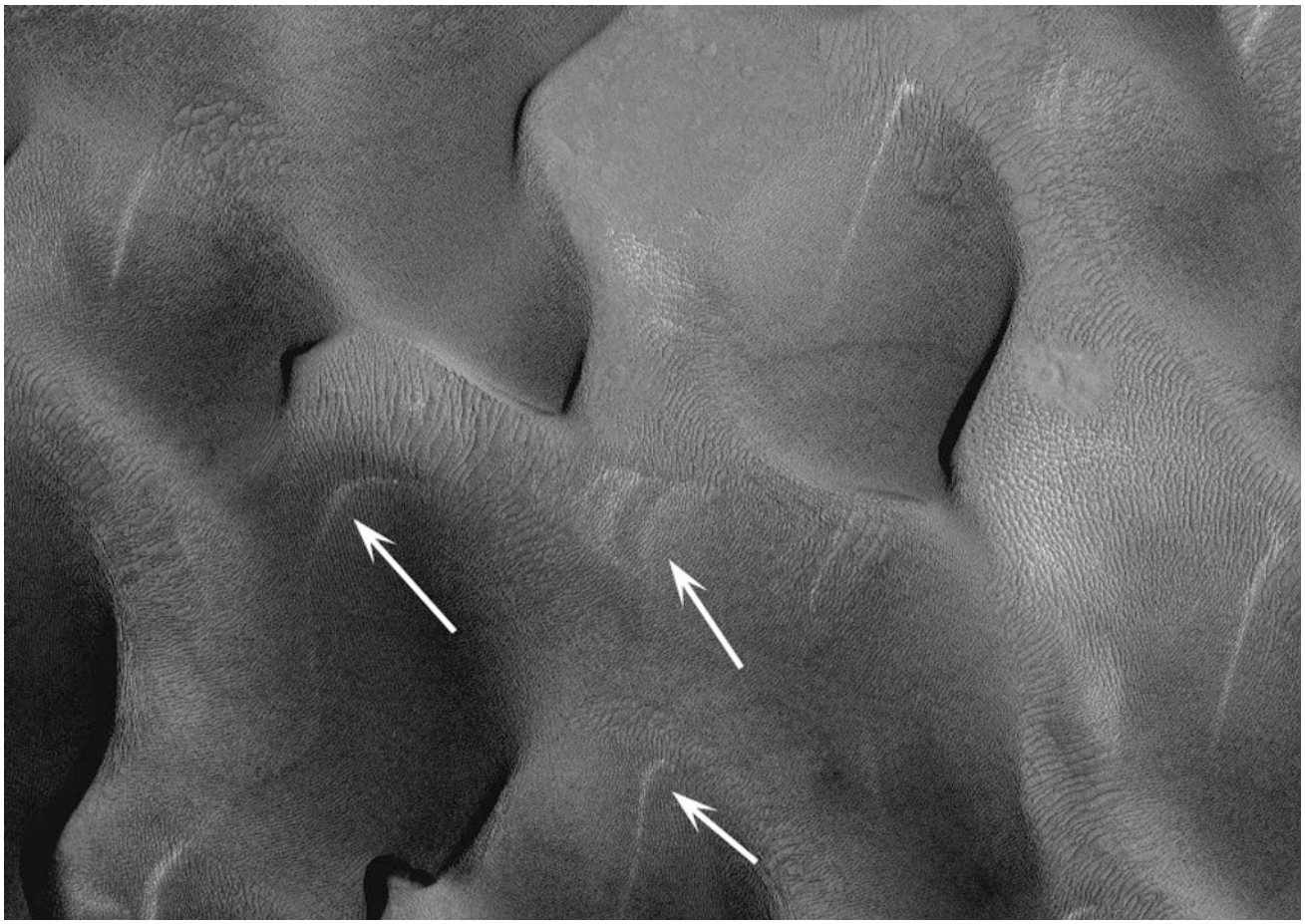

Fig. 5.27 Barchan scars on Mars, seen in HiRISE image PSP_001882_1920 and noted by Gardin et al. (2012). Barchan dunes are readily visible, as are ripples superposed on the dunes and interdune floor. Bright arcuate streaks (*arrowed*) are interpreted as cemented marks of former slip faces—the set of three in the center is particularly indicative of progressive movement of a dune. Those arcs are about 10 m across. Related features are seen on Earth at *White* Sands, and Lencois Maranhenses. *Image* NASA/JPL/U.Arizona

Fig. 5.28 A winter image from a timelapse camera (see Chap. 16) monitoring ripple migration and evolution at Great Sand Dunes National Park and Preserve. After a snowfall, high winds caused ~2 m-wide ripple-like structures to form in the snow—mixed sand and snow transport leads to curling layers visible at *left*. *Image* R. Lorenz

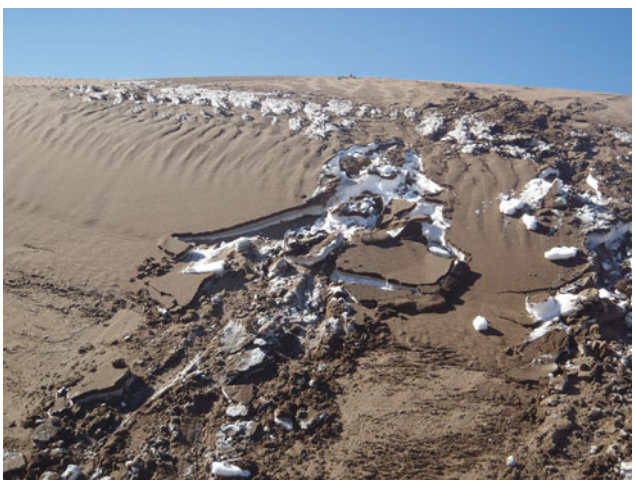

Fig. 5.29 Buried snow layers, literally stumbled upon by the author, on a parabolic dune at Great Sand Dunes National Park and Preserve (Fig. 5.25 was taken on the other side of this dune, about two weeks before this picture was taken). Much of the dune here is rock hard, with moist sand frozen in place. The thickest snow layer here is about 4 cm thick. Note that it is the area where snow is present that has small ripples on the surface, where perhaps the sand mobility has been affected by moisture from the snow. *Photo* R. Lorenz

the last snowfall (Steidtmann 1973). Snow is preserved inside dunes in Alaska and Antarctica (e.g. Bourke et al. 2009).

The phenomenon may not be restricted to the Earth: Mars too may have niveo–aeolian features. The possibility of cementation by moisture was advocated for some time as a possible explanation for why Mars dunes were not observed to move. Although some examples of migration have now been seen (see Chap. 8), the possibility of incorporation of ice in Martian dunes remains. Evidence from orbital neutron spectrometry (Feldman et al. 2008) suggests that the Olympia Undae dunes on Mars contain enough hydrogen (i.e., water) that they may have a substantial ice component.